Shahid Chamran University of Ahvaz

Iranian Association of Electrical and Electronics Engineers

Journal of Applied Research in Electrical Engineering

E-ISSN: 2783-2864
P-ISSN: 2717-414X
Homepage: https://jaree.scu.ac.ir/

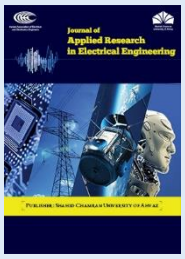

Research Article

Investigating the Effects of Phosphorene Nanotubes (PNTs)-on-Gold Substrates on the Enhancements of the Sensitivity of SPR Biosensors

Amir Davami, Mohammad Hadi Shahrokh Abadi*

Electrical and Computer Engineering Faculty, Hakim Sabzevari University, Sabzevar 9617976487, Iran

** Corresponding Author: mhshahrokh@ieee.org*

Abstract: Surface plasmon resonance (SPR) sensors have been widely considered for their sensitivity, accuracy, and appropriate response speed. This article simulates and analyzes the effects of phosphorene nanotubes (PNTs) layer with various diameters and rolling directions on the structure of SPR biosensor in the Lumerical software environment. The main structure is based on the structure of Kretschmann and the use of the BK_7 prism, a gold (Au) layer, and the end layer of phosphorene nanotubes. The proposed SPR biosensor reflectance curves are obtained, analyzed, and compared for various modes of refractive index n = 1.33 and 1.339, resembling a neutral watery medium and a bacterial medium, respectively. The results show that the minimum reflection is achieved for 30 nm Au at an SPR resonance angle of θ = 71.59° while by adding phosphorene nanotubes, it is observed that at a diameter of 10.08 A and an armchair rolling direction, the configuration on the Au layer becomes favorable. The minimum reflectance of 0.199 is observed for the armchair phosphorene nanotubes (10.08A) layer over 30 nm Au. The combination also provides a sensitivity of 152°/RIU for Δn = 0.009 with a high detection accuracy of 0.079. The results demonstrate that the layer of phosphorene nanotubes has a positive effect on SPR biosensors, and it can be used as a controlling factor in SPR biosensors.

Keywords: Biosensor, phosphorene nanotubes, reflectance, surface plasmon resonance, sensitivity.

Article history
Received 25 December 2021; Revised 01 February 2022; Accepted 04 February 2022; Published online 14 March 2022.

How to cite this article
A. Davami, and M. H. Shahrokh Abadi, "Investigating the effects of phosphorene nanotubes (PNTs)-on-gold substrates on the enhancements of the sensitivity of SPR biosensors," *J. Appl. Res. Electr. Eng.*, vol. 1, no. 2, pp. 169-174, 2022. DOI: 10.22055/jaree.2022.39570.1044

Check for updates

1. INTRODUCTION

Surface plasmon resonance (SPR) is a label-free detection method that has emerged over the past two decades as an appropriate and reliable platform in clinical analysis for biomolecular interactions. The technique can measure interactions in real-time with high sensitivity and without the need for labels. SPR sensors are one of several kinds of optical sensors that measure a variety of biological and chemical parameters according to the interaction between the sample environment and the sensor surface [1-2]. To excite surface plasma at the metal-dielectric interface, the electrons of the metal conduction band must be able to resonate with radiated light on the surface at a given wavelength [3]. There are common methods for exciting surface plasmons, including prism coupling and diffraction grating coupling [1, 4]. The prism coupling is introduced using two different structures, i.e., Krishmann and Otto [5].

In SPR-based biosensors, gold or silver is typically coated directly on the prism to separate the sensor medium and prism. Gold is used as one of the most appropriate materials because of its great resistance to oxidation and its high chemical stability.

However, the capacity of biomolecules to interact with gold is weak, thereby reducing the sensitivity of the sensor. To solve this problem, recent research on biosensor structure has used one or more layers of graphene because of its high surface-volume ratio, high electrical mobility, and stability of its atomic structure [3]. However, it does not act as a semiconductor due to the inadequate bandgap in its electronic structure [6]. This deficiency inhibits its use in many applications, including optoelectronics.

Transition metal dichalcogenides (TMDCs), another important member of the 2D material family, have also generated interest among scientists. Molybdenum disulfide (MoS_2), the most common TMDCs [7], has a perceptible band

gap, allowing the conversion of electrons into light photons and resulting in extraordinary on/off ratios. However, the MoS_2 sandwich structure the mobility of the charge carrier [8].

It seems that phosphorene can be a good alternative because it does not have any of the disadvantages of graphene and TMDCs. Black phosphorus (PB), one of the three main phosphorus allotropes, is the most thermodynamically stable relative to its red and white counterparts. An extraordinary property of black phosphorus is its high mobility [9-13], which is responsible for most of BP's unique electronic properties. Previous studies have shown that low-layer BP has great mobility, ranging from 600 cm^2/V.s to 1000 cm^2/V.s at room temperature [10-12, 14], which makes it possible to apply BP in electrode materials.

In addition, another remarkable property of BP is its direct and tunable bandwidth in single and multi-layer forms [10, 11], making BP an ideal semiconductor for potential applications in extraordinary light emission and effective photoelectric conversion. In addition, because of the low bandgap assigned to the significant excitation binding energy, p-type and n-type configurations can be set in BP to meet the broad range of demands in optoelectric devices, including tubular devices. BP's thin films have received scientific attention from all over the world. The puckered structure provides the BP with anisotropy in the plane, resulting in its thermal conductivity [19] and transportation anisotropy dependent on the single angle [15], particularly in the mobility of carriers [16, 17].

According to the specific properties of black phosphorus, the features of BP nanotubes have attracted more attention [18-20], such as carbon nanotubes. In comparison, research on BP tubes is limited. However, the urgent demand for tubular electronics highlights the importance of research on BP tubes, particularly for their electronic and optical properties. Due to the anisotropy of BP, the rolling direction of BP nanotubes is a decisive factor in their electrical properties.

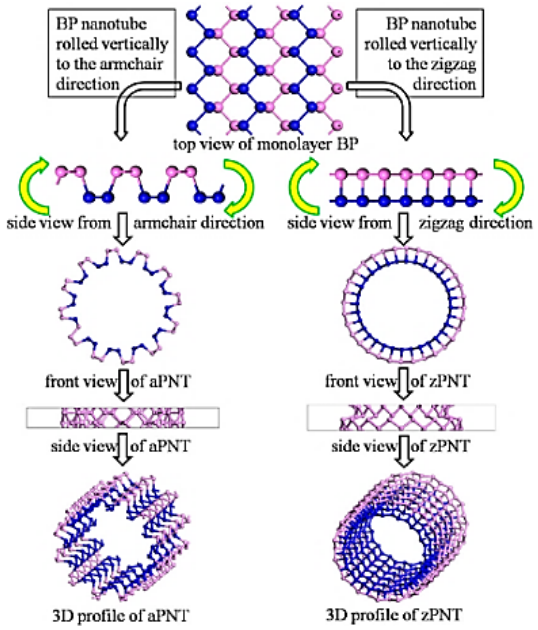

Fig. 1: A schematic diagram of the construction of BP nanotubes [21].

In addition, BP nanotubes' bandgap and optical properties can be modulated by their diameter. Therefore, we systematically investigated the properties of BP nanotubes with two different rolling directions and different radii. Similar to graphene, bulk black phosphorus is a stratified material with atomic layers superimposed by van der Waals interactions. Fig. 1 shows the structure of BP in various side views and a flow chart for the construction of PB nanotubes.

Based on the puckered structure of BP, BP nanotubes are separately rolled vertically to the zigzag or armchair direction to construct the nanotubes known as armchair phosphorene nanotubes (aPNTs) (Fig. 1) and zigzag phosphorene nanotubes (zPNTs). Based on BP's pleated structure, BP nanotubes are separately rolled vertically to the zigzag direction or armchair to construct the nanotubes accordingly [21].

In addition to the rolling direction factor, the curve radius was also taken into account. As a result, BP nanotubes were constructed with different radii of 5.2 A, 7.3 A, 10.06 A, and 11.5 A to analyze the effect of bending stress energy on electronic and optical properties. The radius values are consistent with the median circles of the models, and non-internal values have been chosen to ensure the integrity of the atomic periodicity of the puckered structure [21].

This paper proposes a phosphorene layer with different diameters and rolling directions on the top of an Au layer. The structure is formed as an SPR biosensor at 632 nm incident light, the sensitivity and resonance angle of the biosensor are studied, and the order of the layer is optimized for better resolution. The different structures are then simulated in the Lumerical environment, and changes in the refractive index are studied and compared.

2. The Proposed SPR-Biosensor Structure

2.1. Schematic of the Structure

In this paper, we use a four-layer Krishmann structure, including the prism, gold (Au) layer, phosphorene nanotubes, and the sampling environment, respectively. As shown in Fig. 2, the gold layer is placed on the prism without an intermediary, and the PNT layer is then placed between the Au layer and the sample medium. The physical properties of various simulated materials are presented in Table 1.

2.2. Theoretical Discussion of SPR-Biosensor

Resonance occurs when the tangential component of the incident light wave vector (k_{in}) is equal to the wave vector of the surface plasmons (k_{sp}). The incident light wave vector can increase as much as the surface plasmon wave vector and be excited at a special angle called the surface plasmon resonance angle at the metal–sample interface.

Table 1: Refractive index and thickness of different layers.

Layer	Refractive index	Thickness (or diameter) of PNTs
Prism [22]	1.515	-------
Au [22]	0.185+3.423i	30nm
aPNT(5.2A) [21]	1.3+0.33i	0.52nm
aPNT(7.3A)	1.25+0.41i	0.73nm
aPNT(10.08A)	1.05+0.30i	1.00nm
aPNT(11.5A)	1+0.22i	1.15nm
zPNT(7.3A)	1.43+0.37i	0.73nm
zPNT(11.5A)	1.40+0.22i	1.15nm

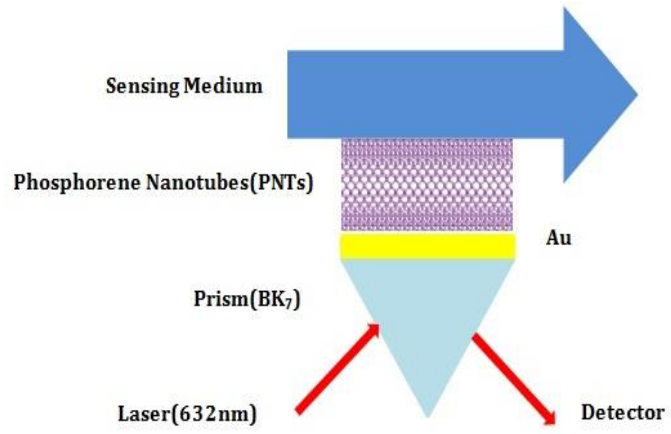

Fig. 2: Illustration of the SPR-biosensor structure.

The resonant angle can be computed by

$$k_{sp} = k_0\sqrt{\left(\frac{\varepsilon_1\varepsilon_2}{\varepsilon_1+\varepsilon_2}\right)} \quad (1)$$

$$\theta_{SPR} = \sin^{-1}\left[\sqrt{\frac{1}{n_p}\left(\frac{\varepsilon_1\varepsilon_2}{\varepsilon_1+\varepsilon_2}\right)}\right] \quad (2)$$

in which ε_1 and ε_2 are the dielectric constant of the metal and the sensor environment, respectively, and n_p is the refractive index of the prism. Assuming resonance and energy transfer from photons to surface plasmons, the intensity of the reflected light is significantly reduced [23, 24]. In general, the characteristic of a reflective wave, including intensity, phase, and polarization under resonance conditions, is entirely dependent on the refractive index of the adjacent medium.

The important parameter in the surface plasmon resonance sensor that reflects the performance of this sensor is sensitivity (S), which indicates the rate of changes in sensor output to the changes in the measured characteristic. For example, in angular modulation, the ratio of the surface plasmon resonance angle variations to the changes in the refractive index of the sensor environment is expressed as

$$S = \frac{\Delta\theta_{SPR}}{\Delta n_s} \quad (3)$$

Detection accuracy (D.A) indicates the proximity of the measured characteristic to its true value and is calculated by

$$D.A = \frac{\Delta\theta_{SPR}}{FWHM}. \quad (4)$$

Finally, the quality factor (Q) is obtained by [25]

$$Q = \frac{S}{FWHM} \quad (5)$$

3. Results and Discussion

The article aims to study a new detection setup with the use of PNT layers on a thin layer of gold to enhance the light absorption capacity of the SPR biosensor and to further improve its sensitivity. The efficiency of the proposed configurations is verified in the Lumerical environment.

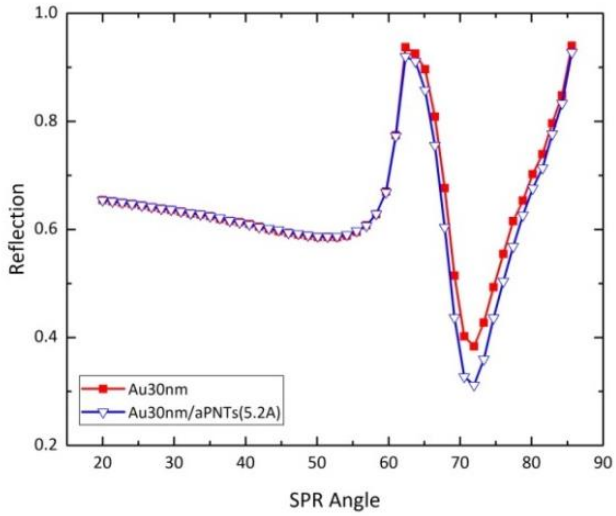

Fig. 3: The reflection spectra curves of the monolayer of Au and aPNTs/Au layers.

As shown in Fig. 3, we first examine the structure with the Au-PNTs, an armchair rolling direction (aPNTs) sensitive layer, and compare it with the results of the gold monolayer at the top of the prism.

The effect of reflected light is examined once in the presence of a gold layer and once again in the presence of aPNTs/Au. Due to the interaction between the incoming light and the surface plasmons of the gold layer, the reflected light will be of minimal intensity at a particular angle. The aim is to find this minimum angle in structures of different thicknesses. The lower the minimum reflection, the more favorable the result will be, indicating that the surface plasmon resonance occurs more strongly. In other words, the incoming light wave vector is perfectly coupled to the surface plasmon on the metal surface.

As can be seen in Fig. 3, the minimum reflectance (R_{min}) in the structure with the Au layer and the thickness of 30 nm is 0.383 and by adding an additional aPNTs layer on 30 nm Au, a ~19% reduction in R_{min} occurs in 0.311 and an approximate difference in SPR angle is $\Delta\theta \approx 0°$. This configuration causes the minimum reflectance to increase dramatically, which is in good agreement with other reports.

By retaining the Au layer thickness at 30 nm, the impact of the additional layer of aPNTs on the minimum reflectance of the aPNTs/30Au configuration was also investigated and compared. As shown in Fig. 4, when the diameter of aPNTs layer grows, the lowest reflectance approaches 0.199 for aPNTs(10.08A)/30Au. Table 2 lists the minimum reflectance's corresponding to the angles of occurrence for the setup simulation at the different diameters of pants layer.

By considering zPNTs/30Au configuration as the optimized reflection spectra and to investigate the effect of zPNTs flakes on the reflection spectra, the diameter of zPNTs layer was increased to 7.3A and 11.5A flakes. Fig. 5 shows that the minimum reflectance does change significantly when the diameter of zPNTs flakes is increased, which has an impact on R_{min}. Details of the values to R_{min} and RA are listed in Table 3.

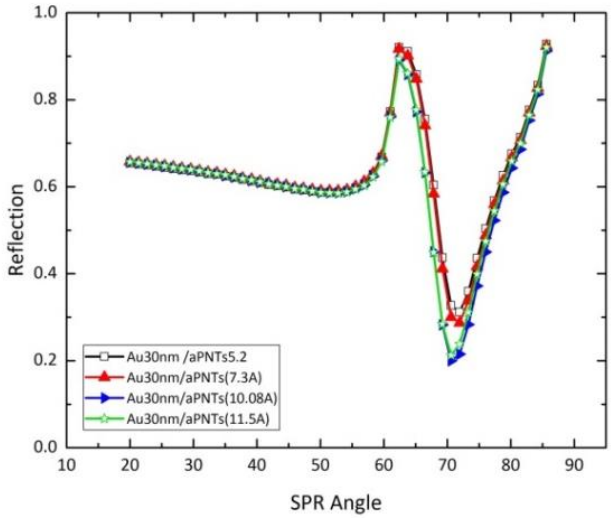

Fig. 4: The reflection spectra for different diameters of aPNTs layers in aPNTs/30Au.

Table 2: Resonance angle (θ°) and Rmin values for different diameters of aPNTs layers in aPNTs/30Au configurations in n = 1.33 environment.

Diameter of aPNTs layer (A)	Resonance angle ($\theta°$)	Minimum reflectance (R_{min})
5.2	71.959	0.311
7.3	71.959	0.287
10.08	70.591	0.199
11.5	70.591	0.212

Table 3: Resonance angle ($\theta°$) and R_{min} values for different diameters of zPNTs layers in zPNTs/30Au configurations in n = 1.33 environment.

Diameter of zPNTs layer (A)	Resonance angle ($\theta°$)	Minimum reflectance (R_{min})
7.3	71.959	0.309
11.5	71.959	0.295

Table 4: The sensitivity (S), detection accuracy (DA), and quality (Q) of the proposed aPNTs(10.08A)/30Au SPR-biosensor versus work in for n = 1.339 medium.

SPR-Biosensor Configuration	aPNTs(10.08A) /30Au	2L_ G/30Au
FWHM	17.23	22.06
Δθ SPR	1.368	6.25
S (°/RUI)	152	89.29
DA	0.079	0.29
Q	8.82	4.26
Reference	This work	[26]

From the results in Figs. 4 and 5, we can see that the minimum reflectance happens at 0.199. This means that the combination of aPNTs(10.08A)/30Au is the most optimal structure among the available configurations. By modifying the medium to n = 1.339, the sensor's sensitivity and the spectral response of the aPNTs (10.08A)/30Au structure are investigated. Fig. 6 indicates the response of the spectral reflection to various environments. Sensitivity, S, can now be

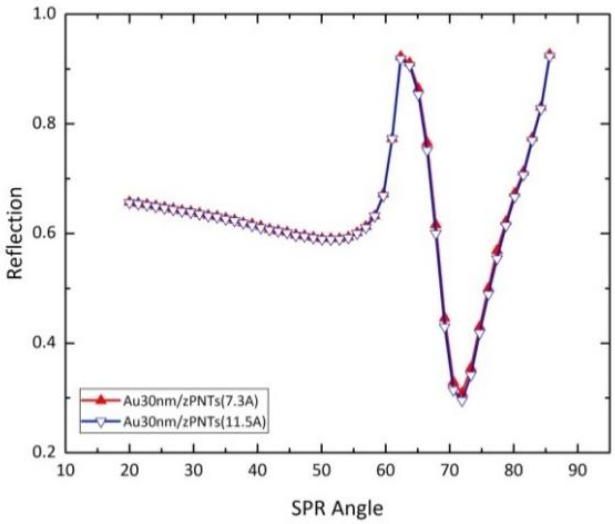

Fig. 5: The reflection spectra for different diameters of zPNTs layers in zPNTs/30Au.

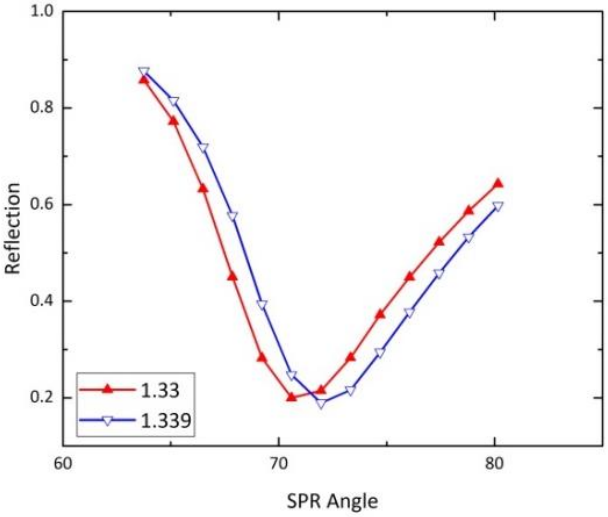

Fig. 6: The reflection spectra for aPNTS(10.08A)/30Au configuration at watery (n = 1.330) and analyte (n = 1.339) representing.

determined using (4) and the details of Fig. 6 in response to n = 1.330 and n = 1.339.

Moreover, FWHM may be estimated at 17.23 based on the results. Equations (3-5) are used to determine sensitivity, detection accuracy, and quality, as listed in Table 5 based on the information in Fig. 5. The results of another investigation [26] into 2L_G/30Au are also presented for comparison.

4. Conclusion

This paper studied and introduced the effect of various PNTs/Au combinations and the diameter of their flakes on the spectral response of an SPR biosensor. In addition, the orders and diameters of the PNT layer and the medium were compared. We also examined the sensor's sensitivity and reflectivity to achieve the best configuration functionality. The results show that aPNTs (10.08A) over 30nm Au have the highest sensitivity of 152°/RIU. The results also show that increasing the diameter of the layers in the outlet has a direct effect on the sensor's efficiency and enhances the sensor's performance.

CREDIT AUTHORSHIP CONTRIBUTION STATEMENT

Amir Davami: Conceptualization, Data curation, Formal analysis, Investigation, Software, Visualization, Roles/Writing - original draft, Writing - review & editing. **Mohammad Hadi Shahrokh Abadi:** Conceptualization, Methodology, Project administration, Supervision, Validation, Visualization, Writing - review & editing.

DECLARATION OF COMPETING INTEREST

The authors declare that they have no known competing financial interests or personal relationships that could have appeared to influence the work reported in this paper. The ethical issues; including plagiarism, informed consent, misconduct, data fabrication and/or falsification, double publication and/or submission, redundancy has been completely observed by the authors.

REFERENCES

[1] Li. Wu, H. S. Chu, W. S. Koh, and E. P. Li., "Highly sensitive graphene biosensors based on surface plasmon resonance," *Optics Express*, vol. 18, no. 14, pp. 14395-14400, 2010.

[2] J. Homola, *Surface plasmon resonance based sensors*. Springer Science & Business Media, vol. 4, 2006.

[3] K.V. Sreekanth, S. Zeng, K. Yong, and T. Yu, "Sensitivity enhanced biosensor using graphene-based one-dimensional photonic crystal," *Sensors and Actuators B: Chemical*, vol.182. pp. 424-428, 2013.

[4] P. K. Maharana, and R. Jha, "Chalcogenide prism and graphene multilayer based surface plasmon resonance affinity biosensor for high performance," *Sensors and Actuators B: Chemical*, vol. 169, pp. 161-166, 2012.

[5] A, Komlev, R. Dyukin, and E. Shutova, "The method of controlling the thickness of the deposited film on the basis of the surface plasmon resonance effect," *Journal of Physics: Conference Series*, 2017, IOP Publishing.

[6] T. H. Wang, Y. Zhu, and Q. Jiang, "Bandgap opening of bilayer graphene by dual doping from organic molecule and substrate," *Journal of Physical Chemistry C*, vol. 117, no. 24, pp. 12873-12881, 2013.

[7] K. S. Yong, D. M. Otalvaro, I. Duchemin, M. Saeys, and C. Joachim, "Calculation of the conductance of a finite atomic line of sulfur vacancies created on a molybdenum disulfide surface," *Physical Review B*, vol. 77, no. 20, 205429, 2008.

[8] M. S. Fuhrer, and J. Hone, "Measurement of mobility in dual-gated MoS 2 transistors," *Nature nanotechnology*, vol. 8, no. 3, pp. 146-147, 2013.

[9] S. I. Allec, and B. M. Wong, "Inconsistencies in the electronic properties of phosphorene nanotubes: new insights from large-scale DFT calculations," *Journal of Physical Chemistry Letters*, vol. 7, no. 21, pp. 4340-4345, 2013.

[10] V. Sorkin, Y. Cai, Z. Ong, G. Zhang, and Y. W. Zhang, "Recent advances in the study of phosphorene and its nanostructures," *Critical Reviews in Solid State and Materials Sciences*, vol. 4, no. 2, pp. 1-82, 2017.

[11] L. Lia, Y. Yu, and G. Ye, "Black phosphorus field-effect transistors," *Nature NanoTechnology*, vol. 9, no. 5, pp. 372-377. 2014.

[12] W. Zhang, J. Yin, P. Zhang, and Y. Ding, "Strain/stress engineering on the mechanical and electronic properties of phosphorene nanosheets and nanotubes," *The Royal Society of Chemistry 2017 advances*, vol. 7, no. 81, pp. 51466-51474. 2017.

[13] W. H. Chen, C. Yu, I. C. Chen, and H. C. Cheng, "Mechanical property assessment of black phosphorene nanotube using molecular dynamics simulation," *Computational Materials Science*, vol. 133, pp. 35-44, 2017.

[14] Y. Deng *et al.*, "Black phosphorus–monolayer MoS2 van der Waals heterojunction p–n diode," *2014 American Chemical Society Nano*, vol. 8, no. 8, pp. 8292-8299. 2014.

[15] C. Gomez *et al.* , "Isolation and characterization of few-layer black phosphorus," *2D Materials*, vol. 1, no. 2, 025001, 2014.

[16] H. Liu, Y. Du, and Y. Deng, "Semiconducting black phosphorus: synthesis, transport properties and electronic applications," *Chemical Society Reviews*, vol. 44, no. 9, pp. 2732-2743, 2015.

[17] P. Yasaei *et al.*, "High-quality black phosphorus atomic layers by liquid-phase exfoliation,"*Advanced Materials*, vol. 27, no. 11, pp. 1887-1892, 2015.

[18] S. Yu, H. Zhu, K. Eshun, A. Arab, A. Badwan, and Q. Li, "A computational study of the electronic properties of one-dimensional armchair phosphorene nanotubes," *Journal of Applied Physics*, vol. 118, no. 16, article 164306, 2015.

[19] T. Hu, A. Hashmi, and J. Hong, "Geometry, electronic structures and optical properties of phosphorus nanotubes, " *Journal of Applied Physics*, vol. 26, no. 41, 2015.

[20] R. Ansari, A. Shahnazari, and S. Rouhi, "Density-functional-theory-based finite element model to study the mechanical properties of zigzag phosphorene nanotubes," *Physica E: Low-dimensional Systems and Nanostructures*, vol. 88, pp. 272-278, 2017.

[21] Z. Xie , Z. Chen, N. Cheng , J. Wang ,and G. Zhu , "Tunable bandgap and optical properties of black phosphorene nanotubes," *Materials*, vol. 11, no. 2, article 304, 2018.

[22] H. Vahed, and C. Nadri, "Sensitivity enhancement of SPR optical biosensor based on Graphene–MoS2 structure with nanocomposite layer," *Optical Materials*, vol. 88, pp. 161-166, 2019.

[23] H. Raether, *Surface plasmons on smooth and rough surfaces and on gratings*. Springer, vol. 118, pp. 4-39, 1988.

[24] K. Choi, H. Kim, and Y. Lim, "Analytic design and visualization of multiple surface plasmon resonance excitation using angular spectrum decomposition for a

Gaussian input beam," *Optics Express*, vol. 13, no. 22, pp. 8866-8874, 2005.

[25] X. Dai, Y. Liang, Y. Zhao, S. Gan, Y. Jia, and Y. Xiang, "Sensitivity enhancement of a surface plasmon resonance with tin selenide (SnSe) allotropes," *Sensors*, vol. 19, no. 1, article 173, 2019.

[26] J. Maurya, Y. Prajapati, and R. Tripathi, "Effect of molybdenum disulfide layer on surface plasmon resonance biosensor for the detection of bacteria," *Silicon*, vol. 10, no. 2, pp. 245-256, 2018.

BIOGRAPHY

Amir Davami received his B.Sc. degree in electrical engineering from Islamic Azad University of Tabriz, Iran in 2011, his M.Sc. degree in Nanoelectronics Engineering from Tabriz University, Iran in 2014. Now, he is an Electrical Engineering Ph.D. student at Hakim Sabzevari University, Iran. His research interests are nanoelectronics, semiconductor technology, and optoelectronic devices.

Mohammad Hadi Shahrokh Abadi has received his B.Sc. in electronics engineering (1994) from the University of Semnan, Iran, and his M.Sc. (2007) and Ph.D. (2010) in Electronics Engineering from the University of Putra Malaysia (UPM). He joined the Department of Electrical and Electronics Engineering, Hakim Sabzevari University, in 2012 as a full-time teacher and researcher in the area of semiconductor devices and materials. He is now Associate Professor at Hakim Sabzevari University, Iran. In 2020, he became a Senior Member of IEEE, where he has joined the organization since 2006. His research areas are not limited to but mainly include semiconductor materials characterization, bending electronics, MOX gas sensors, and biosensors. Currently, he is working on "Wide Band Gap Materials for Solar Cells", "Polymer-Based Solar Cell", "Electronic Biosensor for Detection of Pathogens", and "MOX Gas Sensor for Illicit Drug Detection".